Photodiagnosis and Photodynamic Therapy 25 (2019) 111–118

Contents lists available at ScienceDirect

Photodiagnosis and Photodynamic Therapy

journal homepage: www.elsevier.com/locate/pdpdt

Rose Bengal incorporated to α-cyclodextrin microparticles for photodynamic therapy against the cariogenic microorganism *Streptococcus mutans*

F.J.R. Alexandrino[a,b], E.M. Bezerra[c], R.F. Da Costa[c], L.R.L. Cavalcante[d], F.A.M. Sales[e], T.S. Francisco[c], L.K.A. Rodrigues[f], D.H. Almeida de Brito[g], N.M.P.S. Ricardo[g], S.N. Costa[h], P. de Lima-Neto[i], I.L. Barroso-Neto[j], E.W.S. Caetano[k,*], V.N. Freire[j]

[a] *Departamento de Patologia e Medicina Legal, Programa de Pós-graduação em Microbiologia Médica, Universidade Federal do Ceará, 50430-275 Fortaleza - CE, Brazil*
[b] *Faculdade Paulo Picanço, 60135-218, Fortaleza-CE, Brazil*
[c] *Departamento de Ciências Naturais, Matemática e Estatística, Universidade Federal Rural do Semi-Árido, 59625-900 Mossoró - RN, Brazil*
[d] *Departamento de Bioquímica e Biologia Molecular, Universidade Federal do Ceará, 60440-970 Fortaleza - CE, Brazil*
[e] *Departamento de Ensino, Instituto Federal de Educação, Ciência e Tecnologia do Ceará, Campus de Aracati, 62800-000 Aracati - CE, Brazil*
[f] *Departamento de Odontologia Restauradora, Faculdade de Farmácia, Odontologia e Enfermagem, Universidade Federal do Ceará, 60430370 Fortaleza - CE, Brazil*
[g] *Departamento de Química Orgânica e Inorgânica, Universidade Federal do Ceará, CP 12100, Campus do Pici, 60451-970 Fortaleza - CE, Brazil*
[h] *Departamento de Engenharia Metalúrgica e de Materiais, Programa de Pós-graduação em Engenharia e Ciência de Materiais, Universidade Federal do Ceará, 60440-554 Fortaleza- CE, Brazil*
[i] *Departamento de Química Analítica e Físico-Química, Universidade Federal do Ceará, 60440900, Fortaleza- CE, Brazil*
[j] *Departamento de Física, Universidade Federal do Ceará, Caixa Postal 6030, Campus do Pici, 60440-900 Fortaleza - CE, Brazil*
[k] *Instituto Federal de Educação, Ciência e Tecnologia do Ceará, 60040-531 Fortaleza - CE, Brazil*

ARTICLE INFO

Keywords:
Rose Bengal
α-cyclodextrin microparticles
Photodynamic therapy
Antibacterial activity
Molecular interaction simulations
Antimicrobial photodynamic therapy

ABSTRACT

Rose Bengal@α-cyclodextrin (RB@α-CD) microparticles (μPs) were prepared and the RB inclusion in α-CD was experimentally demonstrated through infrared, UV–VIS absorption spectroscopy and cyclic voltammetry. The RB inclusion in α-CD was theoretically investigated using classical molecular mechanics calculations, the simulation results showing that RB can be included in both the narrow and wide apertures of the α-cyclodextrin ring with configurations exhibiting average binding energies of about 27 kcal mol^{-1}. The prepared RB@α-CD microparticles were characterized through Scanning Electron Microscopy (SEM) and it was demonstrated that they are highly efficient in the photodynamic therapy against a *Streptococcus mutans* (the main bacteria of cariogenic dental plaque) suspension, as a concentration of RB@α-CD μPs 10 times smaller than the usual concentration of pure RB is still capable to produce significant antibacterial activity.

1. Introduction

Photodynamic therapy (PDT) employs the combination of light and chemical substances for the treatment of cancer tumors [1] and to kill harmful microorganisms [2]. The use of nanosized carriers to improve PDT drugs and decrease side effects is an important research trend [3]. In particular, PDT for the treatment for the treatment of oral infections have been proposed. For example, recent results indicate the promising application of Curcumin against oral bacteria, fungi and drug resistant strains using biocompatible vehicles [4]. A chlorophyll derivative presented adequate antimicrobial efficacy for root canal disinfection [5], and the use of PDT combined with the antibiotic clarithromycin against generalized aggressive periodontitis was evaluated very recently [6].

The dye chromophore Rose Bengal (RB - 4,5,6,7-tetrachloro-2′,4′,5′,7′-tetraiodofluorescein), which is commonly used in the Na salt form $C_{20}H_2Cl_4I_4Na_2O_5$, is a well known photosensitizer in photodynamic therapy with a singlet oxygen quantum yield of nearly 76% under 532 nm light irradiation – see Fig. 1(a) [7–10]. However, it was found that the RB immobilization by covalent bonds with substrates decreases its rate of singlet oxygen generation, favouring the use of noncovalent complexes to retain most of its photosensitizer role [11]. Among its good characteristics, RB is inexpensive and biodegradable, has free amino groups (which is attractive for the establishment of new chemical bonds with substrates) and is nontoxic for mammals, having

* Corresponding author at: Departamento de Física, Universidade Federal do Ceará, Caixa Postal 6030, Campus do Pici, 60440-900, Fortaleza, CE, Brazil.
E-mail address: ewcaetano@gmail.com (E.W.S. Caetano).

https://doi.org/10.1016/j.pdpdt.2018.11.016
Received 26 August 2018; Received in revised form 9 November 2018; Accepted 19 November 2018
Available online 20 November 2018
1572-1000/ © 2018 Elsevier B.V. All rights reserved.

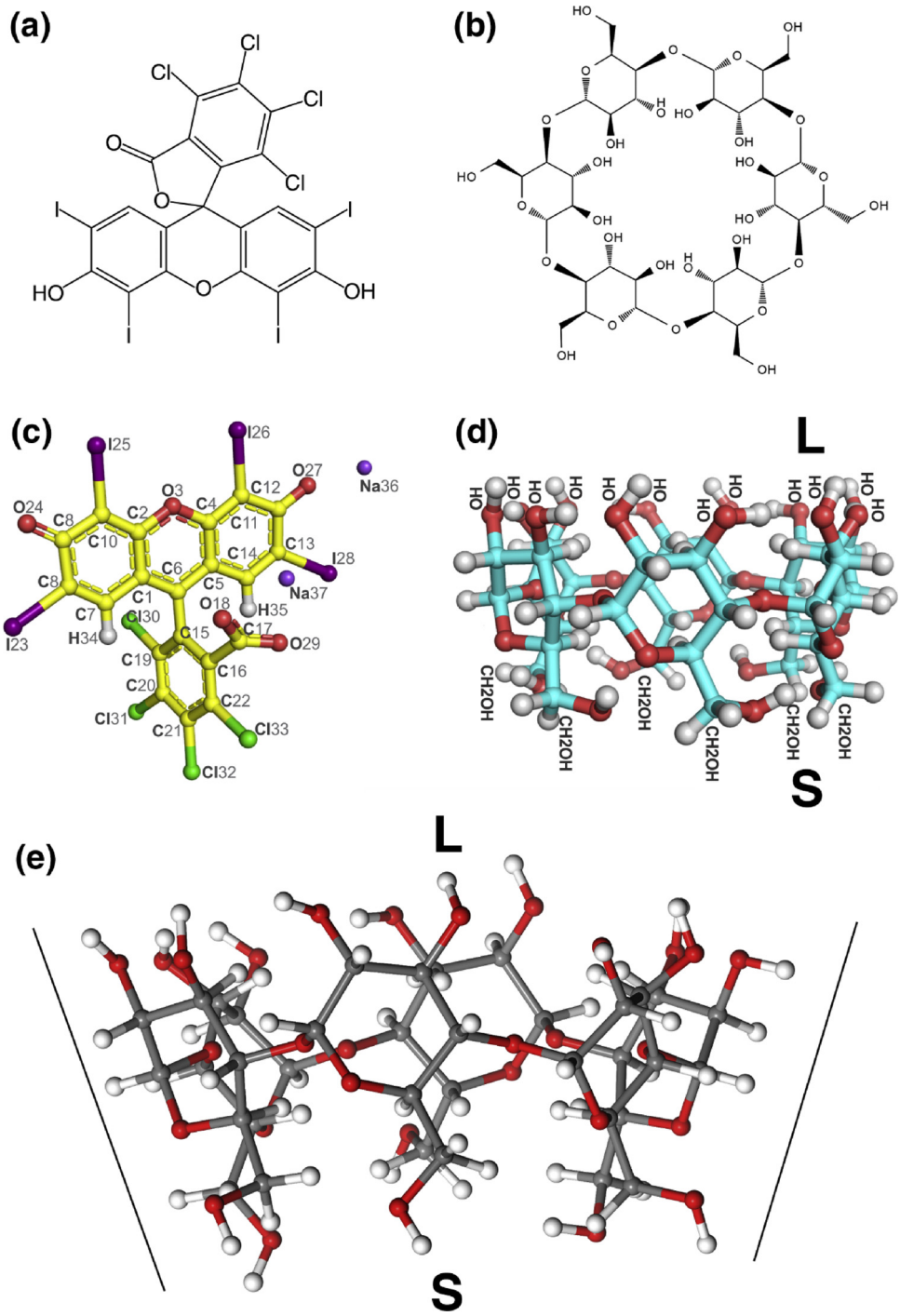

Fig. 1. (a) Rose Bengal and (b) α -cyclodextrin molecular structures. (c) Rose Bengal molecule at physiological pH interacting with Na ions; (d) the α-cyclodextrin (α-CD) molecule depicting the −OH groups / larger cavity (L) and $-CH_2OH$ groups /smaller cavity (S) sides. (e) Representation of cyclodextrin showing its truncated cone shape (see solid lines) and the different sizes of the larger (L) and smaller (S) cavities.

in itself some antimicrobial activity [11]. RB-based photodynamic therapy against *Streptococus mutans* was probed [12,13], but due to its hydrophilic character RB suffers from poor intracellular uptake ability [14]. Concerning this aspect, the use of microparticles for an improved RB delivery is pursued, being supposed that their surfaces modified with RB can have an enhanced antimicrobial effect [15,16]. As a matter of fact, RB was used in silica nanoparticles to inactivate the Gram (+) bacteria *S. epidermidis* and *S. aureus*16], and it was demonstrated that photoactivated RB functionalized chitosan nanoparticles produce antibacterial activity and stabilize dentin-collagen [17]. Besides, bimodal optical diagnostics of oral cancer based on a RB conjugated gold nanorod plataform was proposed [18], as well as RB-conjugated gold nanorods for in vivo photodynamic and photothermal oral cancer therapies [7].

Within the scope of finding new and promising applications of nanomaterials in dentistry [19], we focus attention on the natural cyclodextrins (CDs) for drug delivery and pharmaceutical applications [20–23]. As stated clearly by Lakkakula and Krause [21], natural and modified CDs have been studied and some have gained US FDA approval or achieved 'Generally Regarded as Safe' (GRAS) status. CDs are a family of macrocyclic oligosaccharides formed by six (α-CD, the cheapest one), seven (β-CD, the most widely used) or eight (γ-CD) D-

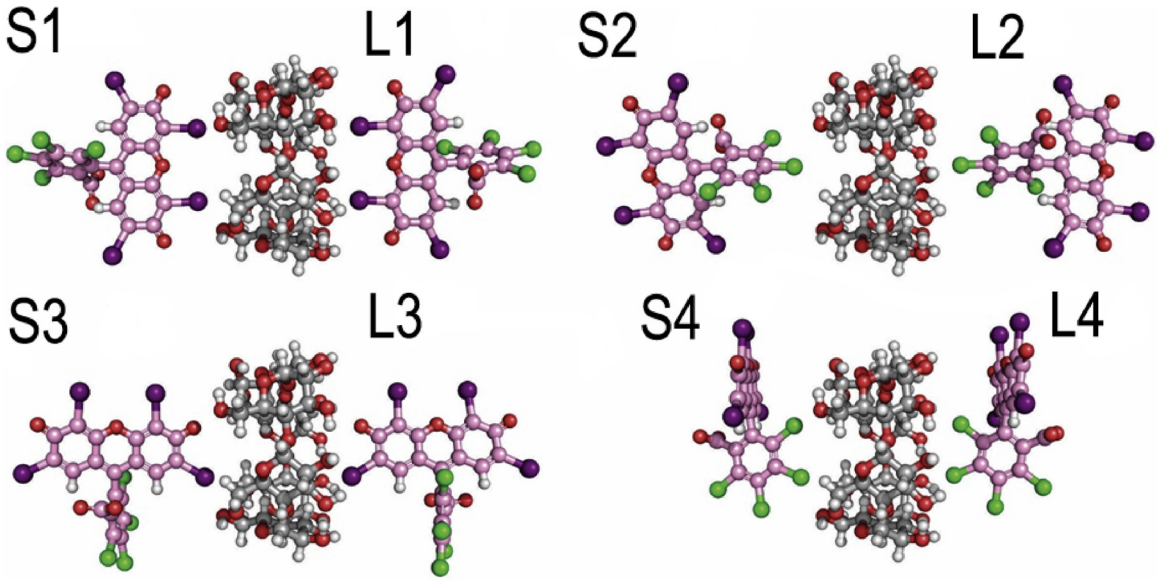

Fig. 2. Initial molecular geometries used to investigate the interaction energy of the Rose Bengal@α-cyclodextrin complex.

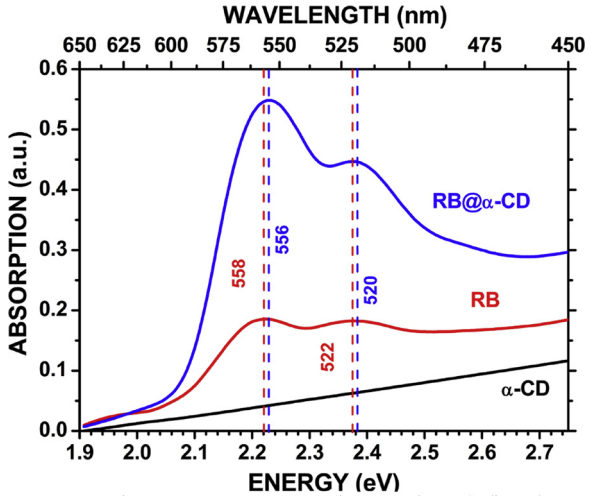

Fig. 3. Optical absorption spectra of α-CD (black line), RB (red), and RB@α-CD (blue) obtained for liquid samples at room temperature with a Hewlett-Packard spectrophotometer, model 8453 Diode-Array.

glucose units linked by α(1→4) glycosidic bonds. This gives rise to the CDs cone-like or barrel-shaped molecular cavities in different conformations having asymmetric extremities: one with −OH groups / smaller aperture (S) / negatively charged, an the other with $-CH_2OH$ groups / larger aperture (L) / positively charged – see Fig. 1 (d and e) [24]. These differences in the CD aperture sizes should promote an asymmetric binding (inclusion, encapsulation) of guest molecules within the host cavity and improve bioavailability of molecular species of pharmaceutical interest, as outlined by Khedkar et al. [25] However, effects of this asymmetric binding due to hydrogen bonding with the −OH and $-CH_2OH$ groups on the molecular delivery by CDs were not described yet to the knowledge of the authors.

It is interesting to highlight that Flamigni [26] has reported that RB binds only to γ-CD, mainly in a 1:1 stochiometric ratio with Kb = 100 $dm^3\,mol^{-1}$. On the other hand, the spectroscopic and electrochemical study of RB in aqueous solutions of CDs performed by Fini et al. [27] indicated that RB forms inclusion complexes only with hydroxypropyl-β-cyclodextrins (HP-β-CD) and hydroxypropyl-γ-cyclodextrins (HP-γ-CD), but not with α-cyclodextrin (α-CD). In another work, lastly, Fini et al. [28] have studied the interaction of Rose Bengal (RB) in aqueous solution of $LiClO_4$ 0.1 mol L^{-1} with four different cyclodextrins, namely hydroxypropyl-β-cyclodextrin (HP-β-CD), hydroxypropyl-γ-cyclodextrin (HP-γ-CD), heptakis(2,6-di-O-methyl)-β-cyclodextrin (DIMEB), and heptakis (2,3,6-tri-O-methyl)-β-cyclodextrin (TRIMEB) by spectrophotometric and calorimetric measurements. Their results suggested that, at the concentration studied, RB is included in all modified CDs forming 1:1 complexes with different stabilities depending on cavity size and kind of derivative. Finally, in a more recent work, Fini et al. [29] have performed a spectroscopic investigation of Rose Bengal/cyclodextrin interactions in aqueous solution for the case of the hydroxypropyl-cyclodextrins, finding evidence of the complex formation between the RB and all HP - α, β, γ CDs both in water and in buffer.

By taking advantage of the good characteristics of RB as a photosensitizer and those of CD for drug delivery outlined in the preceding paragraphs, the proposal of this work is to briefly describe the production and characterization (by UV–vis optical absorption, IR spectroscopy, scanning electron microscopy, cyclic voltammetry) of Rose Bengal @ α-Cyclodextrin microparticles (RB@α-CD), followed by a classical theoretical description of the most important structural characteristics of this inclusion due to the noncovalent RB binding to α-CD at both −OH and $-CH_2OH$ sides.

2. Materials and methods

2.1. RB@α-CD synthesis

In the encapsulation procedure, 1.0 g of α-cyclodextrin was dissolved in 200 mL of distilled water and gently stirred for 4 h at 25 °C. Afterwards, 100 mg of Rose Bengal were added to the solution which was stirred overnight. The solution was used as feed in a spray-dryer equipment Buchi, Switzerland, model B-290 (spray drying is a common encapsulation technique) to obtain Rose Bengal encapsulated in the α -cyclodextrin matrix. The inlet and outlet air temperatures were maintained at 130 °C and 65 °C, respectively, with a feed flow of 3.5 mL/min, an aspirator volume flow of 35 m^3/h, and an air volume flow of 84 L/h. In order to estimate the relative concentration of Rose Bengal per each 10 mg of the RB@ α -CD microparticles the following method was employed: 18 concentrations in the range 2–20 mg/L of RB in double distilled water were prepared. The UV–vis spectra of each solution was obtained with an observed absorption maximum at 558 nm. The relative intensity of this maximum as a function of the RB concentration was linearly interpolated and, afterwards, the optical

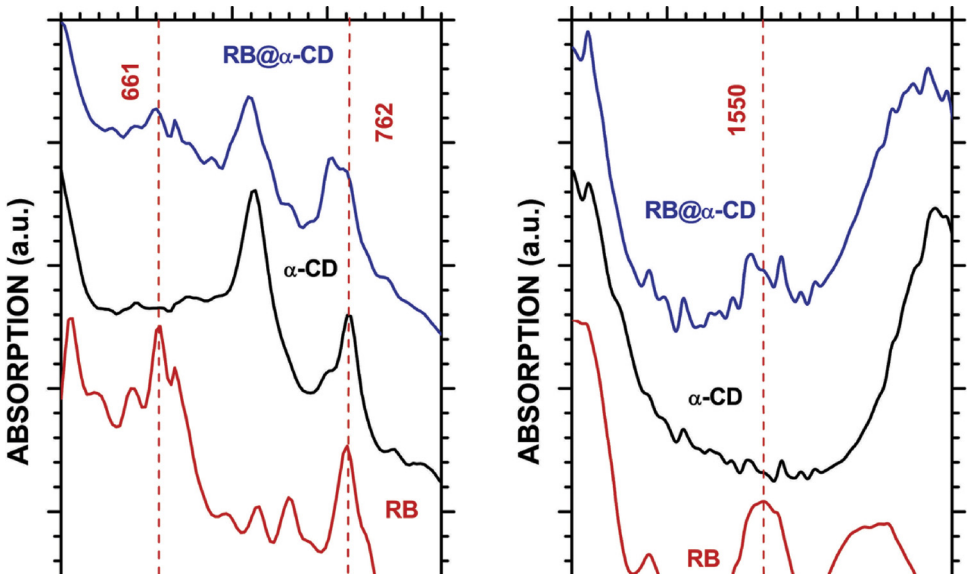

Fig. 4. Infrared absorption spectra of α-CD (black line), RB (red), and RB@α-CD (blue). Solid state samples were used after dispersion, grinding and pressuring with KBr to form a pellet. The spectra were measured using an ABB Bomem FT-IR spectrometer, model 2000-120 FTLA.

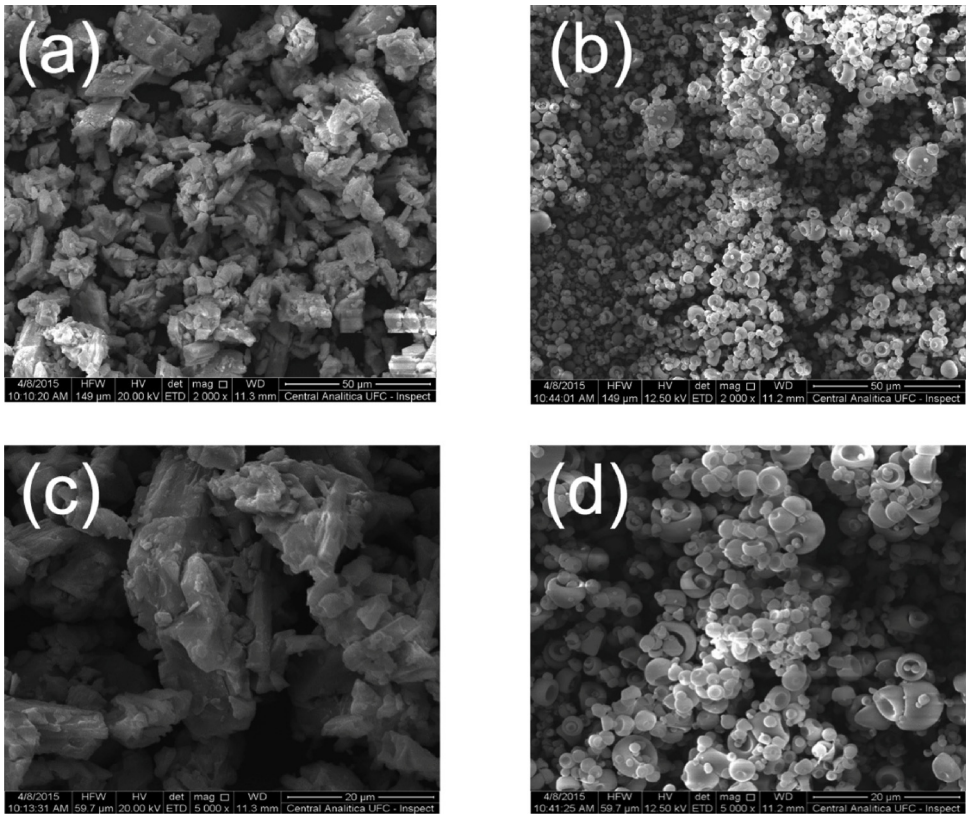

Fig. 5. Morphological aspect of the rose bengal dye pure (a and c) and complexed with alpha-cyclodextrin forming microparticles and microcapsules (b and d).

absorption of an aqueous solution containing 10 mg of RB@ α -CD microparticles was measured at 558 nm as well. Considering that CD does not exhibit optical absorption in this wavelength, the linear interpolation previously obtained, combined with the Lambert-Beer equation, allowed us to obtain the concentration of 1.38 mg of Rose Bengal per each 10 mg of the RB@α-CD microparticles (so 13.8% of the sample mass was due to RB).

2.2. Infrared spectrum

The vibrational spectrum in the infrared region (FTIR) was obtained from samples in solid state, previously dispersed, grinded and pressed with potassium bromide (KBr, 100 mg, 1 wt %) to form a pellet. The spectra were collected through 80 scans at a resolution of 2 cm^{-1}. The absorption measurements were all performed using an ABB Bomem FT-IR spectrometer, model 2000-120 FTLA with spectral window 400 of the 4000 cm^{-1}.

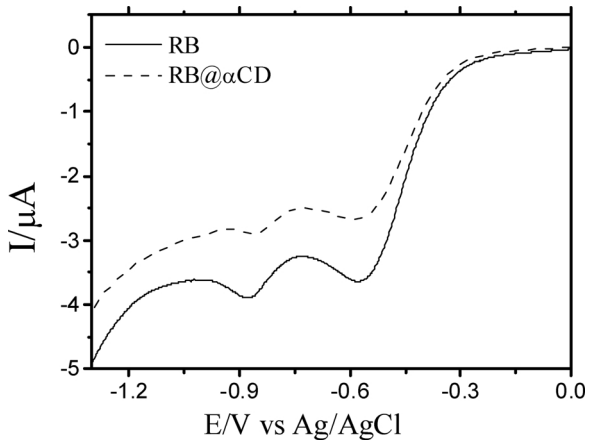

Fig. 6. Voltage-current relationship obtained to 2×10^{-4} mol L^{-1} Rose Bengal on a glassy carbon electrode in presence (dashed line) and absence (solid line) of 5×10^{-2} mol L^{-1} α-cyclodextrin. Both curves were obtained in phosphate buffer solution, at pH 7, at room temperature (≅ 25 °C) and using Potentiodynamic Polarization technique with a scan rate of 10 mV s^{-1}.

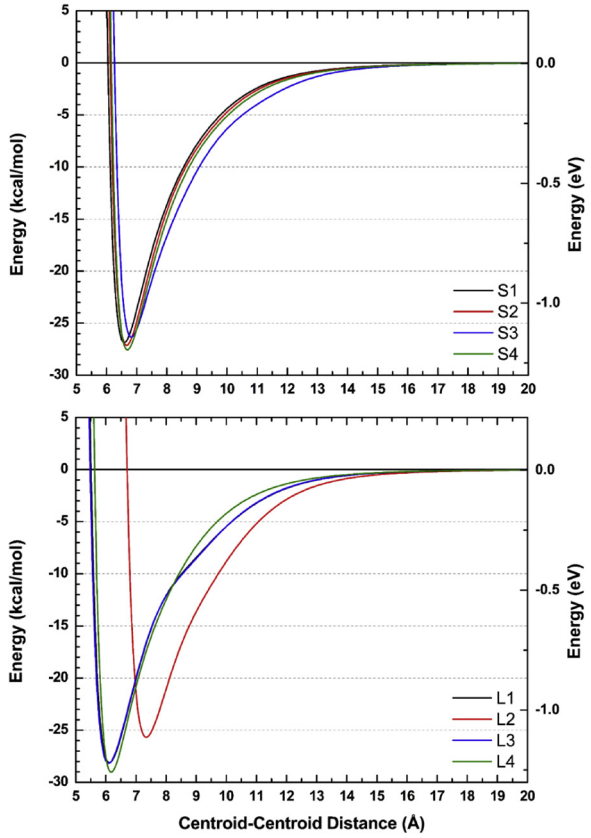

Fig. 7. Interaction energy as a function of the centroid-centroid distance of the RB@α-CD complex obtained for a set of eight optimized configurations, four at the smaller (S1, S2, S3, S4) mouth of α-CD and four at the largest (L1, L2, L3, L4) one. Each geometry was translated rigidly along the centroid-centroid axis.

2.3. UV–vis spectrum

The electronic spectra in the regions of the visible and ultraviolet ranges for samples in aqueous solution were obtained at room temperature with a Hewlett-Packard spectrophotometer, model 8453 Diode-Array. The absorbance was obtained by direct reading of the spectra in the region of 200–800 nm (6.21–1.55 eV) using as blank the solvent NaCl 0.89%.

2.4. Potentiodynamic polarization measurements

The electrochemical potentiodynamic polarization experiments were performed using a Metrohm Autolab PGSTAT 302N potentiostat / galvanostat, controlled by the NOVA program for data acquisition and treatment. All voltammograms were obtained at 10 mV s^{-1} and at room temperature (≅25 °C). A conventional electrochemical cell containing a disc glassy carbon of 3 mm diameter was used as the working electrode, while a 2 cm^2 Platinum foil served as auxiliary electrode and $Ag_{(s)}/AgCl_{(s)}/Cl^-_{(aq.)}$ (saturated KCl) as reference electrode. Phosphate buffers at pH 7 and containing 2×10^{-4} mol L^{-1} of Rose Bengal, with or without 5×10^{-2} mol L^{-1} α-cyclodextrin concentration, were used as working solutions.

2.5. Scanning electron microscopy

The surface morphology of the powder samples (RB and RB@α-CD) were observed using a scanning electron microscope (SEM) (FEI® INSPECT F50). The sputtered gold coated sample were examined and photographed in SEM at an accelerating voltage between 12.50–20.00 kV.

2.6. Biological essays

For the microbiological assay, PDT efficacy against planktonic suspensions of *Streptococcus mutans* was tested with the photosensitizers Rose Bengal (RB) (Sigma-Aldrich, Milwaukee, WI, USA) and Rose Bengal encapsulated with cyclodextrin (RB@α-CD). The preparation for encapsulation was performed in a spray-dryer equipment Buchi, Switzerland model B-290. The inlet and outlet air temperatures were maintained at 130 °C and 65 °C, repectively, with a feed flow of 3.5 mL/min, aspirator volume of 35 m^3/h, and air volume flow of 84 L/h.

The light source used was an Ultrablue plus light emitting diode (LED, λ = 520 nm, DMC, São Carlos, SP, Brazil). Rose bengal has maximum absorption peak around 520 nm. The energy densities used were 3.35 J.cm^{-2}, 6.70 J.cm^{-2} and 10.05 J.cm^{-2}, corresponding to 60 s, 120 s and 180 s of irradiation, respectively. The choice of LED instead of LASER was due to its broader emission band, smaller size, reduced weight and cost of the apparatus, greater flexibility in irradiation time and also ease of handling [30,31]. Specifically, blue LEDs are already used in everyday dental practice, not damaging oral tissues [13]. In PDT, LED light only has demonstrated absence of antimicrobial action [32,33].

The bacterial inoculum was prepared as follows: a standardized suspension of *S. mutans* UA 159 (ATCC 700610) was obtained for uptake of the microorganism. First, Tryptone Soy Broth (TSB, Becton, Dickinson and Company, Sparks, MD 21152 USA) enriched with 0.5% yeast extract (Becton, Dickinson and Company, Sparks, MD 21152 USA) and 1% glucose (Fina Química, Rio de Janeiro, RJ, Brazil) was inoculated with *S. mutans* and then incubated for 18 h at 37 °C in a 5% CO_2 atmosphere (Thermo Fischer Scientific, Model 311, OH 45750, Marietta, Ohio, USA). The suspension was adjusted to 1–2 × 10^6 CFU to perform assays employing broth microdilution technique in order to find out the minimum inhibitory concentration (MIC), according to the procedures specified by the Clinical Laboratory Standards Institute (CLSI, 2012). For this assay, stock solutions with initial concentrations of 32 μmol L^{-1} RB and 64 μmol L^{-1} of RB@α-CD and 11 binary dilutions of each photosensitizer were tested on 96-well microplates (Techno Plastic Products, TPP®, Switzerland). The microplates were incubated at 37 °C and 5% CO_2 for 24 h. Minimum inhibitory concentration was considered to be the lowest concentration of photosensitizer (RB or RB@α-CD) capable of inhibiting the growth of *S. mutans* observed by visual inspection (absence of visible turbidity) and absorbance reading of 492 nm (Thermoplate, Tp-Reader-Basic New, CHINA). The determination of the minimum bactericidal concentration (MBC) was performed afterwards. MBC was defined as the minimum

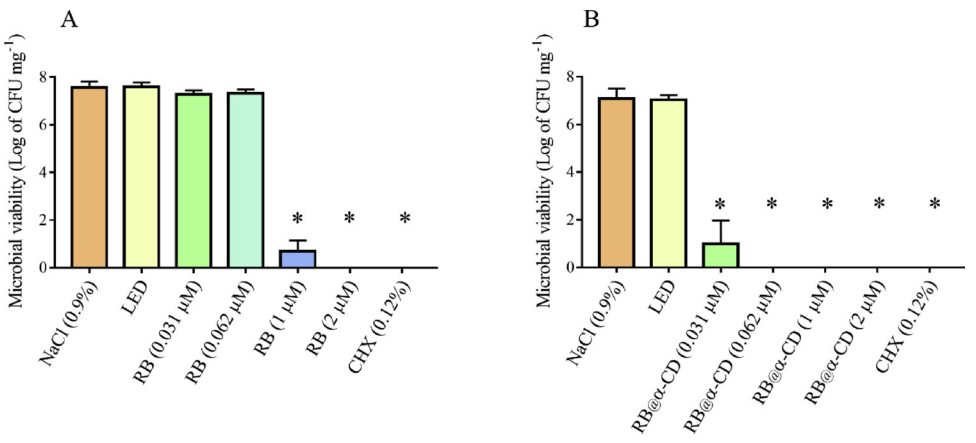

Fig. 8. Microbial viability (log of CFU/mL) of *Streptococcus mutans* after Rose Bengal (RB)/ Rose Bengal encapsulated with cyclodextrin (RB@α-CD) activation using blue light for 60 s (3.35 J.cm $^{-2}$). (A): Microbial viability of *S. mutans* suspensions after exposure to RB (0,031 µmol L^{-1}; 0,062 µmol L^{-1}; 1 µmol L^{-1} and 2 µmol L^{-1}). (B): Bacterial viability of *S. mutans* suspensions after exposure to RB@α-CD (0,031 µmol L^{-1}; 0,062 µmol L^{-1}; 1 µmol L^{-1} and 2 µmol L^{-1}). Control groups: NaCl 0.9%, LED (blue light at 3.35 J.cm^{-2}) and Chlorhexidine (CHX) 0.12%. *indicates significant differences ($p < 0.05$) when compared to the LED only exposure control. Each bar represents the mean ± SD triplicate values.

concentration of photosensitizers RB and RB@α-CD required to kill most (≥99.9%) viable microorganisms after incubation. The bacterial viability test, taking the MIC and MBC values for each photosensitizer used, was then performed. For this assay, the microbial suspension was adjusted in broth in order to obtain a concentration of 10^8 CFU/mL. The experimental groups and control groups (negative control groups- NaCl 0.9%, with and without LED activation, and a positive control group with Chlorhexidine 0.12%) were analyzed in triplicates.

The colony-counting data were transformed to Log CFU. Statistical analysis was performed using Student's *t*-test and ANOVA followed by Tukey's test. In cases where the data showed some asymmetry, the nonparametric Wilcoxon and Friedman tests followed by Dunn's post hoc method were employed. In all situations, the maximum significance level adopted for affirmative findings was 95% ($p < 0.05$). Statistical analyzes were performed using the GraphPad Prism 7.0 software (GraphPad Software, San Diego, CA, USA).

2.7. Classical molecular mechanics calculations

Adsorption simulations of a single Rose Bengal molecule complexed to α-cyclodextrin were performed using classical molecular mechanics. Eight distinct conformations of Rose Bengal placed near to the smaller (outer ring with $-CH_2OH$ groups, S1, S2, S3, S4) and larger (outer ring with $-OH$ groups, L1, L2, L3, L4) cavities of the α-cyclodextrin molecule were evaluated as shown in Fig. 2. In a first moment, the total energy of the Rose Bengal@α-cyclodextrin (RB@α-CD) systems were optimized using the Universal force field (UFF) [34]. The resulting structures were afterwards subjected to a classical annealing calculation using the Forcite code. A total of 100 annealing cycles were performed with minimum and maximum temperatures of 200 K and 300 K, respectively, with 50 heating ramps and 100 steps of 1 fs per ramp in a canonical (NVT) ensemble. The temperature was monitored with a Nosé thermostat. At the end of the annealing cycles, the best molecular geometry for each initial conformer were again optimized and used as inputs to evaluate the adsorption potential, as described in reference [29].

The adsorption energy of each molecule complexed to cyclodextrin was defined as the energy difference between the RB@α-CD system and the energy of each component (RB, α-CD) optimized separately. The adsorption energy as a function of the centroid-centroid distance between RB and α-CD for each conformation was evaluated. The following convergence thresholds were adopted for the classical molecular mechanics computations: energy variation between two successive steps smaller than 2.0×10^{-5} kcal. mol^{-1}, force per atom smaller than 0.001 kcal mol^{-1}. Å^{-1}, and maximum displacement smaller than 1.0×10^{-5} Å.

3. Results and discussion

Fig. 3 shows the optical absorption spectra of α-CD, RB and the RB@α-CD optical absorption curves in the 1.90–2.75 eV energy range. The α-CD curve exhibits a practically uniform linear increase, while RB has two humps, one at 558 nm (2.22 eV) and another at 522 nm (2.37 eV). Semi-empirical calculations using the ZINDO approach [30] suggest that the first peak can be assigned to transitions between a molecular ground state with strong π-like HOMO character and a first excited state with dominant contribution from the π-like LUMO molecular orbital, both located at the carbon rings bound to the iodine atoms. The second transition, on the other hand, involves a transition between the HOMO π-like ground state and the LUMO + 3 σ-like second excited state, which is also located at the iodine bound carbon rings. For the RB@α-CD microparticles, the UV-VIS spectral curve is very similar to the curve for pristine RB, with a small redshift of only 2 nm, probably due to the weak non-covalent interaction of RB with α-CD.

The infrared absorption spectrum of α-CD, RB and the RB@α-CD is depicted in two wavenumber ranges in Fig. 4, the first between 610 and 810 cm^{-1} (left) and the second between 1450 and 1650 cm^{-1} (right). Three vibrational signatures of the RB IR absorption can be seen at 661 cm^{-1}, 762 cm^{-1}, and 1550 cm^{-1} which correspond to peaks also observed in the RB@ α-CD complex. The maximum at 661 cm^{-1} can be assigned to an out-of-plane deformation of the benzene ring bound to the chlorine atoms and the scissors motion of the O—C–O group attached to it. At 762 cm^{-1}, there is a RB peak with a very close absorption band for α-CD assigned to the bending of the CH_2OH groups. The corresponding RB normal mode consists in an out-of-plane motion of all its benzene-like parts and the wagging of the O—C–O group. Finally, the RB peak at 1550 cm^{-1} corresponds to C—C and C–O bond stretchings at the central benzene ring with one oxygen atom and to C—C vibrations of its neighbor rings bound to the iodine species. Overall, one can describe the RB@α-CD IR absorption curve as the superposition of both the RB and α-CD spectra, this being due to the non-covalent nature of their interaction.

Fig. 5 shows the morphology of pure RB (a, c) and RB complexed with α-CD (RB@α-CD) through scanning electron microscopy. While pure RB exhibits microcrystals with apparent sharp edges and sizes above 20 µm, the spray dryed RB@α-CD powder shows the formation of spherical microparticles and microspheres with diameters ranging from 1 to 8 µm, which is the typical powder morphology obtained through the synthesis process we used here [36,37]. Besides, reports point to the formation of cyclodextrin aggregates with diameters frequently less than about 300 nm in aqueous solution in the presence of other compounds [38,39], a process which certainly promotes the formation of the spherical microparticles and microcapsules of RB@α-CD observed in our SEM measurements.

The interaction between the Rose Bengal and the α-cyclodextrin

was evaluated by Potentiodynamic Polarization technique and the voltammetric curves obtained in presence and in absence of α-cyclodextrin are displayed in Fig. 6. In this figure, it can be noted that Rose Bengal presents two peaks at the cathodic sweep, indicating that this molecule receives electrons from electrode, promoting its electrochemical reduction on glassy carbon electrode. In addition, the decrease of both peaks currents values in presence of α-cyclodextrin, reveals the existence of some interaction between Rose Bengal with α-cyclodextrin. This result differs from that presented by Fini et al. [40] that did not observe any effect of including α-cyclodextrin in their peak current measurements, although a small shift was observed when α-CD was added in aqueous media with RB, possibly due to changes in the polarity of the chromophore environment (batochromic effect) produced by interaction between the polar aqueous media and the apolar cyclodextrin cavity.

Fig. 7 shows the interaction energy profile of a single molecule of rose bengal complexed with a single molecule of α-cyclodextrin according to classical molecular mechanics calculations. The interaction energy was plotted as a function of centroid-centroid distance with both molecules being displaced along an axis perpendicular to the α-cyclodextrin ring. When RB is placed near to the small mouth ($-CH_2OH$ groups attached) of α-CD, we obtain, for distinct relative orientations (S1, S2, S3, S4, see Fig. 2) very similar interaction energy curves, with minimum energy of about -27 kcal mol^{-1} (-1.4 eV) for a distance between centroids within the 6.5–6.8 Å range. On the other hand, for the large mouth placement ($-OH$ groups, L1, L2, L3, L4), three of the curves (L1, L3, and L4) are very close to each other, with energy minimum between -28 and -29 kcal mol^{-1} (the later for L4, with the three fused iodine-benzene rings parallel and the tetrachloring ring perpendicular to the cyclodextrin plane) and centroid-centroid distance in the 6–6.3 Å interval. The minimum for the L2 case (the rose Bengal molecule placed perpendicularly to the cyclodextrin large mouth with the tetrachlorine ring closer), in contrast, occurs at about 7.3 Å with energy of about -26 kcal.mol^{-1}. These results suggest that there is a relatively strong non-covalent binding of rose bengal to α-cyclodextrin, supporting our experimental results.

Prevention of dental caries is traditionally performed through the mechanical removal or non-specific control of dental plaque. The use of antimicrobial agents acts in a complementary way to the mechanical control of the plaque [41]. The oral cavity, inhabited by more than 1.000 different bacterial species and containing 10^8-10^9 bacteria/mL of saliva demands strategies that ideally prevent plaque biofilm formation without affecting its biological balance to control the disease [42]. As chlorhexidine (chlorhexidine digluconate 0.12%) is the antimicrobial agent of choice for inhibition of the formation of cariogenic biofilms, we have used it as a positive control of this study [43].

On the other hand, photodynamic therapy (PDT) is a valuable tool in the control of dental plaque bacteria [44–47]. One of the advantages of bacterial death by the activation of photosensitizers by light is that the resistance to the action of singlet oxygen is unlikely to occur, compared to the experience with traditional chemical antimicrobial agents such as antibiotics [48]. Complexation by cyclodextrins usually produces changes in the physicochemical properties of photosensitizing molecules, particularly in their photoreactivity [49]. The chromophore of the dye or photosensitizer included in the cyclodextrin cavity finds a relatively hydrophobic environment and is often able to form hydrogen bonds with cyclodextrin [50]. In addition, the presence of the cyclodextrins in solution may be useful in preventing dye self-aggregation and its photooxidation, thus being able to avoid a decrease in dye efficiency through hydrophobic interactions [51].

In Fig. 8, we present the results of our microbial viability experiments using pure Rose Bengal and Rose Bengal encapsulated within α@-cyclodextrin. The minimum inhibitory concentration (MIC) value for RB activated by LED at an energy density of 3.35 J.cm^{-2} was 1 μmol L^{-1} and the minimum bactericidal concentration (MBC) was 2 μmol L^{-1}. For RB@α-CD, the MIC and MBC values under the same irradiation conditions were 0.031 μmol L^{-1} and 0.062 μmol L^{-1}, respectively. The photodynamic therapy exhibited a significant reduction in bacterial viability for both photosensitizers (RB and RB@α-CD) in the plankton cell suspension model and different irradiation times ($p < 0.05$). The reduction of the bacterial viability, observed by the action of both photosensitizers, did not suffer interference from the times tested (60 s, 90 s and 120 s), so only the results for a 60 s exposure are shown. After exposure of *S. mutans* to 2 μmol L^{-1} of RB or 0.062 μmol L^{-1} of RB@α-CD no more microbial growth in PDT was observed ($p < 0.05$).

The large efficiency improvement of encapsulated RB against the bacteria probably results from an increase of RB intake through bacterial membranes due to the encapsulation substrate (one can note that a 0.031 μmol L^{-1} concentration is 10 times smaller than the usual concentration of pure RB capable to produce significant antibacterial activity). The systems containing encapsulated photosensitizers, as a matter of fact, have several advantages over non encapsulated photosensitizing molecules, including (i) a higher critical mass for the production of reactive oxygen species; (ii) a limitation on the ability of the target cell to pump the drug molecule out, thereby reducing the possibility of multiple drug resistance; (iii) treatment selectivity via localized release of the agents, which can be obtained through passive or active targeting on the charged surface of the inclusion complexes; and (iv) the non immunogenic character of the matrix [52]. According to Paulino et al. [53], the application of RB at concentrations below 5.0 μmol L^{-1} in the dark was not toxic to fibroblasts. Therefore, the concentrations used in this work (0.031 μmol L^{-1}, 0.062 μmol L^{-1}, 1 μmol L^{-1} and 2 μmol L^{-1}) do not exert cytotoxicity on human cells and may be applicable in future *in vivo* studies.

4. Conclusions

In summary, we have produced microparticles of α-cyclodextrin (α-CD) with rose Bengal (RB) for use against the bacteria *S. mutans* through photodynamic therapy, which has a significant role in the process of tooth decay. UV-VIS optical absorption and infrared spectroscopy measurements were carried out to characterize the formation of the RB@α-CD complex, as well as classical molecular mechanics simulations to investigate their interaction. A non-covalent interaction between the dye and the microparticle was identified due to a small (2 nm) wavelength deviation in the optical absorption spectrum, which exhibited features characteristic of RB. The infrared absorption curve of RB@α-CD, on the other hand, clearly revealed three peaks due to RB at 661, 762 and 1550 cm^{-1}. The morphology of pure RB and RB@α-CD was assessed through scanning electron microscopy (SEM), with the pure RB sample exhibiting sharp edge microcrystals larger than 20 μm, and RB@α-CD sample revealing the formation of spherical microparticles and microspheres with diameters in the 1–8 μm range. Potentiodynamic Polarization measurements produced voltammetric curves for pure RB and RB@α-CD microparticles, with the RB curve exhibiting two cathodic peaks larger than those obtained for RB@α-CD, indicating an interaction between Rose Bengal and α-cyclodextrin. The classical molecular mechanics calculations showed that the binding centroid-centroid distance of RB to α-CD is within the 6–7.5 Å range, with binding energies between 26 and 29 kcal mol^{-1}, with the strongest binding corresponding to a single RB placed at the largest mouth of α-CD with its tethraclorine ring perpendicular to the α-CD ring and the three fused iodine-benzene rings parallel to the cyclodextrin ring. Finally, and most important, an investigation of the effectivity of the RB@α-CD microparticle system on the viability of bacterial samples has revealed that for concentrations 10 times smaller than the usual for RB use against S. mutans, the irradiation of RB@α-CD microparticles leads to the complete eradication of the bacteria.

Acknowledgements

The authors would like to thank the Brazilian Research Agency CNPq for financial support. This study was also financed in part by the Coordenação de Aperfeiçoamento de Pessoal de Nível Superior - Brasil (CAPES) - Finance Code 001. E. W. S. C. received financial support from CNPq project 304781/2016-9. E. M. B received financial support from Universal-CNPq project 456432/2014-0. R. F. C received financial support from Universal-CNPq project 455959/2014-5. N. M. P. S. Ricardo received financial support from CNPq project 307837/2017-3 and would like to thank Central Analítica at UFC for allowing her to perform the SEM measurements in their installations.

References

[1] D.E.J.G.J. Dolmans, D. Fukumura, R.K. Jain, Nat. Rev. Cancer 3 (2003) 380–387.
[2] M.R. Hamblin, T. Hasan, Photochem. Photobiol. Sci. 3 (2004) 436–450.
[3] E. Paszko, C. Ehrhardt, M.O. Senge, D.P. Kelleher, J.V. Reynolds, Photodiagnosis Photodyn. Ther. 8 (2011) 14–29.
[4] C. Santezi, B.D. Reina, L.N. Dovigo, Photodiagnosis Photodyn. Ther. 21 (2018) 409–415.
[5] P. Diogo, M. Mota, C. Fernandes, D. Sequeira, P. Palma, F. Caramelo, M.G.P.M.S. Neves, M.A.F. Faustino, T. Gonçalves, J.M. Santos, Photodiagnosis Photodyn. Ther. 22 (2018) 205–211.
[6] N.M.R.B. Andere, N.C.C. dos Santos, C.F. Araújo, I.F. Mathias, A. Rossato, A.C. de Marco, M. Santamaria Jr, M.A.N. Jardini, M.P. Santamaria, Photodiagnosis Photodyn. Ther. 24 (2018) 115–120.
[7] B. Wang, J.-H. Wang, Q. Liu, H. Huang, M. Chen, K. Li, C. Li, X.-F. Yu, P.K. Chu, Biomaterials 35 (2014) 1954–1966.
[8] E. Gandi, Y. Lion, A. Van de Vorst, Photochem. Photobiol. 37 (1983) 271–278.
[9] R.W. Redmond and J.N. Gamlin, 1999, 70, 391- 475.
[10] T. Zhao, X. Shen, L. Li, Z.P. Guan, N. Gao, P. Yuan, S. Yao, Q.-H. Xu, G.Q. Xu, Nanoscale 4 (2012) 7712–7719.
[11] C. Spagnul, L.C. Turner, R.W. Boyle, J. Photochem. Photobiol. B 150 (2015) 11–30.
[12] J.P.M.L. Rolim, Ma S. de-Melo, S.F. Guedes, F.B. Albuquerque-Filho, J.R. de Souza, Na.P. Nogueira, I.C.J. Zanin, L.K. a Rodrigues, J. Photochem. Photobiol. B 106 (2012) 40–46.
[13] C.A. Pereira, A.C.B.P. Costa, C.M. Carreira, J.C. Junqueira, A.O.C. Jorge, Lasers Med. Sci. 28 (2013) 859–864.
[14] E. Fischer, F. Varga, Acta Physiol. Acad. Sci. Hung. 54 (1979) 89–94.
[15] D.K. Chatterjee, L.S. Fong, Y. Zhang, Adv. Drug Deliv. Rev. 60 (2008) 1627–1637.
[16] Y. Guo, S. Rogelj, P. Zhang, Nanotechnology 21 (2010) 065102.
[17] A. Shrestha, M.R. Hamblin, A. Kishen, Nanomed. Nanotechnol. Biol. Med. 10 (2014) 491–501.
[18] J.H. Wang, B. Wang, Q. Liu, Q. Li, H. Huang, L. Song, T.Y. Sun, H. Wang, X.F. Yu, C. Li, P.K. Chu, Biomaterials 34 (2013) 4274–4283.
[19] A. Besinis, T. De Peralta, C.J. Tredwin, R.D. Handy, ACS Nano 9 (2015) 2255–2289.
[20] A. Chordiya Mayur, K. Senthilkumaran, J. Pharm. Pharm. Sci. 1 (2012) 19–29.
[21] Lakkakula Jaya Raju, Macedo Krause Rui Werner, Nanomed. Lond. (Lond) 9 (2014) 877–894.
[22] G. Crini, Chem. Rev. 114 (2014) 10940–10975.
[23] P. Jan Sook, N. Ogawa, T. Loftsson, Int. J. Pharm. 535 (2018) 272–284.
[24] M. Tafazzoli, M. Ghiasi, Carbohydr. Polym. 78 (2009) 10–15.
[25] J.K. Khedkar, V.V. Gobre, R.V. Pinjari, S.P. Gejji, J. Phys. Chem. A 114 (2010) 7725–7732.
[26] L. Flamigni, J. Phys. Chem. 97 (1993) 9566–9572.
[27] P. Fini, M. Castagnolo, L. Catucci, P. Cosma, A. Agostiano, Thermochim. Acta 418 (2004) 33–38.
[28] P. Fini, F. Longobardi, L. Catucci, P. Cosma, A. Agostiano, Bioelectrochemistry 63 (2004) 107–110.
[29] P. Fini, L. Catucci, M. Castagnolo, P. Cosma, V. Pluchinotta, A. Agostiano, J. Incl. Phenom. Macrocycl. Chem. 57 (2007) 663–668.
[30] I.C.J. Zanin, M.M. Lobo, L.K.A. Rodrigues, L.A.F. Pimenta, J.F. Hofling, R.B. Gonçalves, Eur. J. Oral Sci. 114 (2005) 64–69.
[31] K. Konopka, T. Goslinski, J. Dent. Res. 86 (2007) 694–707.
[32] L.S. Peloi, R.R.S. Soares, C.E.G. Bionda, V.R. Souza, N. Hioka, E. Kimura, J. Biosci. (Rajshari) 33 (2008) 231–237.
[33] L.N. Dovigo, A.C. Pavarina, E.G.O. Mima, E.T. Giampaolo, C.E. Vergani, V.S. Bagnato, Mycoses 54 (2011) 123–130.
[34] A.K. Rappe, C.J. Casewit, K.S. Colwell, W.A. Goddard, W.M. Skiff, J. Am. Chem. Soc. 114 (1992) 10024–10035.
[36] B.-K. Wan, L.-F. Siow, J. Food Process Eng. 40 (2017) e12407.
[37] E.C. Frascareli, V.M. Silva, R.V. Tonona, M.D. Hubingera, Food Bioprod. Process. 90 (2012) 413–424.
[38] A. Ryzhakov, T.D. Thi, J. Stappaerts, L. Bertoletti, K. Kimpe, A.R.S. Couto, P. Saokham, G.V.D. Mooter, P. Augustijns, G.W. Somsen, S. Kurkov, S. Inghelbrecht, A. Arien, M.I. Jimidar, K. Schrijnemakers, T. Loftsson, J. Pharm. Sci. 105 (2016) 2556–2569.
[39] J. Stappaerts, T.D. Thi, E. Dominguez-Vega, G.W. Somsen, G.V.D. Mooter, P. Augustijns, Int. J. Pharm. 529 (2017) 442–450.
[40] P. Fini, R. Loseto, L. Catucci, P. Cosma, A. Agostiano, Bioelectrochemistry 70 (2007) 44–49.
[41] P.C. Baehni, Y. Takeuchi, Oral Dis. 9 (2003) 23–29.
[42] F.J. Van Der Ouderaa, J. Clin. Periodontol. 18 (1991) 447–454.
[43] J. Autio-Gold, Oper. Dent. 33 (2008) 710–716.
[44] S. Wood, D. Metcalf, D. Devine, C. Robinson, J. Antimicrob. Chemother. 57 (2006) 680–684.
[45] A.H. Teixeira, E.S. Pereira, L.K. Rodrigues, D. Saxena, S. Duarte, I.C.J. Zanin, Caries Res. 46 (2012) 549–554.
[46] M.A. Melo, J.P. Rolim, I.C. Zanin, E.B. Barros, E.F. Da-costa, L.K. Rodrigues, Photomed. Laser Surg. 31 (2013) 105–109.
[47] L.G.O. Ricatto, L.A.L. Conrado, C.P. Turssi, F.M.G. França, R.T. Basting, F.L.B. Amaral, Eur. J. Dent. 8 (2014) 509–514.
[48] A.J. MacRobert, S.G. Bown, D. Phillips, Ciba Found. Symp. 146 (1989) 4–12.
[49] M. Nowakowska, M. Smouloch, D. Sendor, J. Incl. Phenom. Macrocycl. Chem. 40 (2001) 213–219.
[50] M.V. Rekharsky, Y. Inoue, Chem. Rev. 98 (1998) 1875–1918.
[51] P.K. Zarzycky, H. Lamparczyk, J. Pharm. Biomed. Anal. 18 (1998) 165–170.
[52] Y.E.L. Koo, W. Fan, H. Hah, H. Xu, D. Orringer, B. Ross, A. Rehemtulla, M.A. Philbert, R. Kopelman, Appl. Opt. 46 (2007) 1924–1930.
[53] T.P. Paulino, P.P. Magalhães, G. Thedei Jr, A.C. Tedesco, P. Ciancaglini, Biochem. Mol. Biol. Educ. 33 (2005) 46–49.